


Simultaneous impact modified and chain extended glass fiber reinforced poly(lactic acid) composites: Mechanical, thermal, crystallization, and dynamic mechanical performance

John Olabode Akindoyo^{1,2}  | Mohammad Dalour Hossen Beg³ | Suriati Ghazali³ | Hans Peter Heim² | Maik Feldmann² | Mustapha Mariatti¹

¹School of Materials and Mineral Resources Engineering, Universiti Sains Malaysia, Seberang Perai, Malaysia

²Institute of Materials Engineering, University of Kassel, Kassel, Germany

³Faculty of Chemical and Natural Resources Engineering, Universiti Malaysia Pahang, Kuantan, Malaysia

Correspondence

John Olabode Akindoyo, School of Materials and Mineral Resources Engineering, Universiti Sains Malaysia, Engineering Campus, 14300 Nibong Tebal, Seberang Perai, Malaysia.
Email: blessedbode@gmail.com

Funding information

Hessen State Ministry of Higher Education, Germany; Universiti Sains Malaysia

[Correction added on 1 March 2021, after first online publication: The copyright line was changed.]

Abstract

Herein, glass fiber (GF) reinforced binary, ternary, and quaternary poly(lactic acid) (PLA) composites were prepared. Toughening, and chain extension of PLA was achieved through the incorporation of impact modifier and chain extender and their concurrent effects on the spectroscopic, crystallization, mechanical, thermal, and thermomechanical properties of the composites were investigated. High mechanical properties of GF influenced the mechanical performance of the composites. However, GF alone could not restrict the chain mobility of PLA due to poor interface and low crystallization activities in the PLA-GF composite. Incorporation of impact modifier and chain extender produced significantly enhanced interaction between GF and PLA. Significantly, the crystallinity, impact strength, and flexural modulus of PLA in the quaternary composite were increased by 58%, 63%, and 66%, respectively. In addition, damping and effectiveness coefficient of the PLA-GF composite were notably reduced by the simultaneous impact modification and chain extension of the reinforced composites.

KEYWORDS

composites, extrusion, mechanical properties, thermal properties, thermoplastics

1 | INTRODUCTION

The excessive dependence on petroleum-based products has resulted in an increasing demand for, and unsustainable consumption of petroleum resources. This has triggered significant depletion of the petroleum reserve and it is generating increasing levels of environmental pollution because the production, use, disposal, and recycling of petroleum-based products generates a lot of greenhouse emission.^{1–3} Therefore, in order to achieve sustainable development of the world we live in, it becomes highly necessary to develop high performance biobased materials or biopolymers to

substitute the existing petroleum-based materials.⁴ Particularly, efforts are being concerted towards the development of renewable and sustainable environment benign materials which could help to maintain the integrity of the environment. Specifically, composites produced from biobased, renewable and biodegradable polymers are currently being widely investigated. Among the several possibilities, one of the notable polymers in the market today that is produced from renewable resource and is known to be very versatile is poly(lactic acid) (PLA).⁵

PLA, which is among the most notable thermoplastic biopolymer, has an aliphatic polyester structure. It is

This is an open access article under the terms of the Creative Commons Attribution License, which permits use, distribution and reproduction in any medium, provided the original work is properly cited.

© 2020 The Authors. *Journal of Applied Polymer Science* published by Wiley Periodicals LLC.

mainly produced from fully renewable resources such as sugar and cornstarch,⁶ and it has considerably high levels of strength and stiffness. In addition, PLA has good biocompatibility, biodegradability, and desirable UV stability.^{7,8} Due to these salient features, PLA is very important to applications such as food packaging, textile and biomedical, and it is potentially suitable for several other structural and technical applications. Therefore, the demand for PLA is widely increasing and it is envisaged that by 2020, the global production capacity of PLA will reach about 800,000 ton/year.⁹ However, PLA has some peculiar shortcoming including its inherently brittle nature, poor thermal resistance, and its considerably low long-term use temperature due to its relatively low glass transition temperature.^{5,10,11} Actually, it has been reported that the major cause of the low toughness and poor thermal resistance of PLA is its low crystallization ability.¹⁰ These shortcomings tend to limit the wide application of PLA, especially in fields where high thermal resistance and toughness are required. Therefore, in order to further extend the potential applications of PLA, it is highly necessary to a deliberately enhance or the performance of PLA, through micro- or macro-modifications.¹² It is well known that polymer matrices can be effectively strengthened through fiber reinforcements whereas improved toughening can be achieved by the use of rubbery additives.¹³ However, it is still a challenge to concurrently enhance the toughness and strength of PLA and this necessitates further investigations.

The reinforcing fibers used for PLA can be classified into natural and synthetic fiber.¹⁴ Although natural fibers generally offer higher environmental friendliness compared to synthetic fiber, but they have relatively poorer strength and it is also more difficult to disperse natural fibers in PLA due to their higher polar nature compared to synthetic fibers.¹¹ Due to this, natural fiber reinforced PLA composites often manifest unsatisfactory mechanical performance especially in terms of ductility and toughness.^{15,16} This often necessitates surface modification, especially to improve interfacial bonding and fiber dispersion.^{17,18} On the other hand, synthetic fibers have stronger mechanical properties than natural fibers and PLA composites reinforced with synthetic fibers have been reported to show far superior mechanical performance compared to natural fiber reinforced PLA composites.^{19,20} Some of the notable synthetic fibers suitable for use with PLA include glass fiber (GF), carbon fibers, and carbon nanotubes. Among these, GF is more commonly used as reinforcement in polymer composites based on its great mechanical performance, desirable heat resistance and more importantly, it is cheaper compared to carbon fiber, which may be otherwise used.^{21–23} Specifically, while 50 cm³ of carbon fiber costs about 150 USD,

50 cm³ of GF cost just about 75 USD.²³ In addition, silicate, borate, and phosphate-based GFs have been observed to possess great biological activity, which makes them suitable for the production of fully degradable composites.²⁴ Notwithstanding, the literature have revealed that the performance of GF reinforced composites is highly dependent on factors such as the aspect ratio of fiber, fiber distribution, fiber content, and fiber-matrix interactions.^{25,26}

In addition to the shortcomings earlier outlined for PLA, another major issue with its processing is the tendency to degrade during processing as a result of thermal degradation and hydrolysis. This has been observed to result in undesirable outcomes, especially the deterioration of physical and mechanical performance due to decreased molecular weight, which in turn limits its potential use in some important applications.^{27,28} Incorporation of chain extenders is often used to restore the molecular weight of PLA, through reactive functionalization of the degraded end groups of the polymer chains. In fact, the effect of chain extenders on the performance of PLA especially in terms of its melt behavior, rheology, processability, and crystallinity has been reported in the literature.^{5,29,30} On the other hand, the toughness of PLA composites has been successfully improved by the addition of rubbery additive and impact modifiers.^{13,31} However, to the best of the authors' knowledge, there are no reports on the possible effects of simultaneous GF reinforcement, impact modification and chain extension of PLA in reinforced PLA composites, especially as it relates to the interface, mechanical performance, crystallinity, and thermomechanical performance of the resulting composites. Interestingly, proper knowledge on this could help to open potential applications as well as expand the existing possible applications of PLA in structural and engineering composites. Therefore, in this contribution, binary, ternary, and quaternary GF reinforced PLA composites were prepared. In order to improve the toughness of PLA, and to reduce thermal degradation due to chain scission, compatible impact modifier (Biomax Strong [BS]) and chain extender (CESA-extend) were deliberately incorporated into the GF reinforced PLA composite in order to investigate the effects of concurrent impact modification and chain extension on the performance of the reinforced PLA composite.

2 | MATERIALS AND METHODS

2.1 | Materials

The matrix used in this study is PLA. The 3052D NatureWorks Ingeo™ Biopolymer is an injection molding PLA grade with molecular weight, $M_w = 139,000$ g/mol,

melt flow index rate of 30–40 g/10 min at 190°C and 2.16 kg load. In addition, the PLA has a density of 1.25 g/cm³ and melting temperature 160–170°C. The reinforcing filler used is CS 7952 E-glass fiber. The E-glass short fiber, which was supplied by Lanxess AG, Cologne (Germany), has a fiber length of 4.5 mm and diameter of 14 μm.

Toughness and impact properties of PLA were modified by incorporating Biomax[®] Strong 120 impact modifier. The impact modifier was kindly supplied by Dupont, Switzerland. In addition, a functional chain extender was incorporated into the quaternary composite. The chain extender (CESA-extend), which was kindly supplied as a solid masterbatch by Clariant GmbH consists of a carrier polymer which commercial PLA, and a functional constituent (Joncryl ADR43685) produced by BASF SE. This functional constituent is an epoxidized styrene-acrylic copolymer, which enhances its thermodynamic miscibility with PLA and Biostrong. It should be noted that GF, BS, and CESA will mostly be henceforth used to represent GF, Biostrong, and CESA-extend in this article.

2.2 | Methods

2.2.1 | Preparation of composites

The different category of composites were prepared by incorporating the predetermined amount (wt%) of GF and other additives such as BS and CESA into the PLA matrix to obtain binary (PLA and GF), ternary (PLA, GF, and BS), and quaternary (PLA, GF, BS, and CESA) composites, respectively. These were analyzed and compared with neat the PLA sample. The different materials were initially dried in a TORO-systems TR-Dry-Jet EASY 15 air drier after which a Leistritz ZSE 18 HPE twin screw extruder ($D = 18$ mm, $L/D = 40$) was used to mix and compound the materials.

In order to facilitate homogeneous mixing and to reduce fiber breakage due to the high shear associated with the first few sections of the barrel, the GF was side-fed into the compounder after the PLA (and other additives, in the case of the ternary and quaternary composite) have been premelted. This was then followed by mixing and homogenization. The extruded composite strand from the extruder was cooled on a discharge conveyor and was cut into uniform length of about 3 mm, using a strand pelletizer (Scheer SGS 25-E). The dried pellets were then fed into an Arburg allrounder 320 C golden edition injection molding machine to prepare the composite test specimens. The operation conditions during the extrusion and injection molding processes are given in Table 1. In order to ease the comparisons, the

amount of GF in the composites was fixed at 10 wt% while the additives such as BS and CESA were fixed as 5 wt% each. The compositions of the different specimens prepared with their code names are given in Table 2.

2.2.2 | Fourier transform infrared spectroscopy

Fourier transform infrared (FTIR) spectroscopy was used to investigate the possible formation of bonds between PLA and the other components of the composites prepared. This functional groups analysis was performed by using a Shimadzu (IR affinity-1S) FTIR spectrometer to generate the IR spectra through the standard KBr technique, over a wavelength range of 400–4000 cm⁻¹.

2.2.3 | Tensile test

The tensile testing was performed on composite test samples prepared according to EN ISO 527, using a universal testing machine (Zwick/Roell Z010). The samples were dried and conditioned at 23°C (50% relative humidity), and the test was performed at a crosshead speed of 5 mm/min. The tensile strength (TS) and tensile modulus (TM) were obtained as an average value of seven replicate samples.

2.2.4 | Flexural test

The test specimens for flexural test were prepared according to EN ISO 178 and the test was performed on a Zwick/Roell Z010 universal testing machine. During the flexural testing, the machine was running at a crosshead speed of 10 mm/min and the flexural samples were conditioned as described for the tensile test samples. The flexural strength (FS) and flexural modulus (FM) were recorded as the average value of seven replicate specimens.

2.2.5 | Charpy impact test

The Charpy impact testing of the different category of specimens was performed according to EN ISO 179-1. Un-notched samples were tested on an impact testing machine (Zwick Charpy impact machine) at a test speed of 2.93 m/sec, using a 1 J hammer. The impact strength (IS) for each specimen category was obtained as an average value from seven replicate specimens.

Extrusion		Injection molding		
Screw speed	200 rpm	Screw speed	150 rpm	
Profile	Temperature (°C)	Profile	Unit	Value
Feeding zone	110	Feeding zone	(°C)	50
Zone 1	165	Compression zone	(°C)	165–185
Zone 2	165	Metering zone	(°C)	190
Zone 3	170	Nozzle	(°C)	185
Zone 4	170	Mold	(°C)	35
Zone 5	175	Screw speed	(rpm)	150
Zone 6	175	Screw position	(mm)	30
Zone 7	170	Injection pressure	(bar)	550–600
Die	170	Holding pressure	(bar)	500–550
		Injection time	(s)	0.50
		Cooling time	(s)	30

TABLE 1 Extrusion and injection molding profiles used to compound and to produce test specimens

Sample code	PLA (wt%)	GF (wt%)	BS (wt%)	CESA (wt%)
PLA	100	—	—	—
PLA-G	90	10	—	—
PLA-GB	85	10	5	—
PLA-GBC	80	10	—	5

TABLE 2 Composition of the different samples and their code names

Abbreviations: GF, glass fiber; PLA, poly(lactic acid).

2.2.6 | Scanning electron microscopy

After tensile testing, scanning electron microscope (SEM, Camscan Electron Optics, Model-MV2300) was used to observe the fractured surface morphology of the samples composite. Prior to SEM observation, the samples were first dried in order to avoid electrical discharges after which they were coated with a thin layer of gold through sputtering, so as to make them conductive.

2.2.7 | Thermogravimetric analysis

Thermal stability of the different samples was investigated through thermogravimetric analysis (TGA) analysis. The TGA analysis was performed using a TA analyzer (TGA Q500 V6.4, Germany). The sample for TGA analysis was placed in a platinum crucible, and the analysis was carried out in a nitrogen atmosphere. The gas flow rate is 40 ml/min) and the samples were heated from room temperature to 800°C at 10°C/min.

2.2.8 | Differential scanning calorimetric analysis

Calorimetry analysis (differential scanning calorimetry [DSC]) was used to determine the glass transition temperature (T_g), crystallization temperature (T_c), and melting temperature (T_m) of the different samples prepared. The analysis was performed in a DSC Q1000 TA instrument. The DSC thermogram was obtained by heating the samples at a constant rate of 10°C/min over a temperature range of 20 to 250°C. The DSC data were further used to determine the degree of crystallinity (X_{DSC}) of PLA in the composite using the heat of fusion of the tested sample and a reference 100% crystalline PLA sample. The X_{DSC} of PLA in the different samples was calculated as described in Equation (1).

$$\% \text{crystallinity } (X_{DSC}) = \frac{\Delta H}{\Delta H_m W} \times 100\%, \quad (1)$$

where ΔH , ΔH_m , and W represents the heat of fusion of the samples (obtained from the DSC analysis), the heat of fusion of the reference 100% crystalline PLA, and the

mass fraction of the matrix, respectively. The heat of fusion (ΔH_m) of the reference 100% crystalline PLA was set at 93.6 J/g.³²

2.2.9 | Dynamic mechanical analysis

The dynamic mechanical properties of PLA and the different composite categories were investigated through dynamic mechanical analysis (DMA). The DMA analysis was performed on a Q800 Dynamic Mechanical Analyzer. During the analysis, the test specimen was placed under dynamic load at a frequency of 1 Hz from -60 to 130°C at a rate of $3^\circ\text{C}/\text{min}$, in a single cantilever mode (amplitude: $20\ \mu\text{m}$). The length of the cantilever was 35 mm and the cross-section of the specimens was $10\ \text{mm} \times 4\ \text{mm}$.

3 | RESULTS AND DISCUSSION

3.1 | Morphological properties

The SEM images of the fractured surface of the samples after tensile testing are presented in Figure 1. As can be seen in Figure 1(a), the surface morphology of neat PLA is smooth which is characteristic of brittle materials. In

addition, no GF is evident in the image in Figure 1(a) because the image represents the unreinforced PLA. On the other hand, the images in Figures 1(b–d) reveal the presence of GF in the composites. Specifically, the image in Figure 1(b) represents the fractured surface of the binary (PLA-G) composite while the image in Figure 1(c,d) represents the fractured surfaces of the ternary (PLA-GB) and quaternary (PLA-GBC) composites, respectively. The image of the binary composite (PLA-G) exhibits several debonding sites while revealing several pull out fibers with smooth surface. This is an indication of poor interaction between the PLA matrix and the GF. However, it is evident from the image that the dispersion of GF within the PLA matrix is relatively uniform. It is well known that the properties of composite materials depend on several factors such as preparation method, dispersion of filler, and filler-matrix interfacial interactions.^{11,31} Therefore, despite the weak interaction, between GF and PLA as revealed by the SEM image in Figure 1(b), the introduction of GF through a side feeder into the extruder barrel as explained in Section 2.2.1 might have helped to facilitate the dispersion of GF in the PLA matrix. Interestingly, this is essential to enhance the mechanical properties of the resulting composites.¹⁰

Incorporation of BS resulted in reduction in the volume of fiber pull-out and debonding sites (Figure 1(c)), perhaps due to improved interaction between the fiber

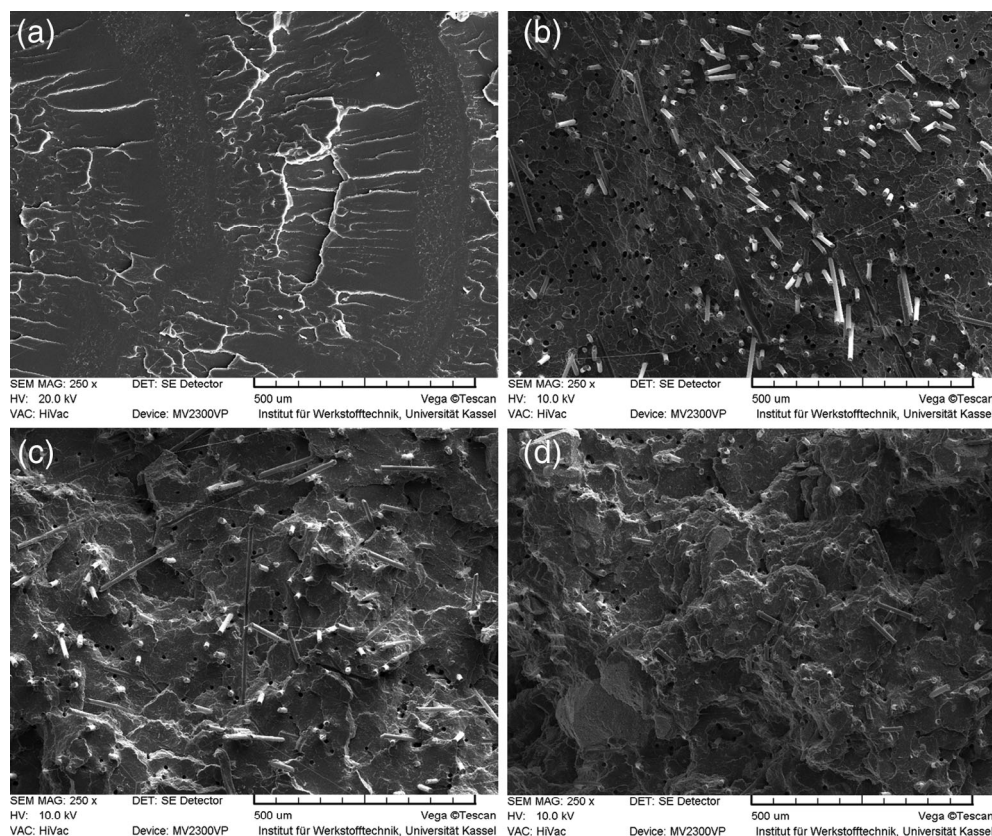


FIGURE 1 Scanning electron microscopic images of the fractured surface (a) neat PLA, (b) glass fiber (GF) reinforced poly(lactic acid) (PLA) composite (PLA-G), (c) GF reinforced ternary PLA composite containing BS (PLA-GB), and (d) reinforced quaternary PLA composite containing BS and CESA (PLA-GBC)

and the matrix. Presence of BS might have helped to lubricate the PLA chains, thereby facilitating good mechanical interlocking such that the grip of PLA on the GF becomes more firm. This would make it difficult for the fiber to easily pull out of the matrix during testing. Invariably, this would influence the performance of the resulting composite. On the other hand, the incorporation of CESA into the ternary system helped to produce notable reduction in the debonding, and pull out of fiber from the matrix as evident through the very low debonding sites and pull out fibers in Figure 1(d). As can be seen, Figure 1(d) reveals more of fiber breakages than fiber pull out. In addition, the few pull out fibers are covered with a thin material layer, which is an indication of improved interaction between the fiber and matrix. Compared to Figure 1(c), the image in Figure 1(d) shows that there is an increased interaction between the filler and the matrix. The resultant effect of this on the performance of the composite is discussed in the subsequent sections.

3.2 | Mechanical properties

The tensile and flexural properties of neat PLA and the binary (PLA-G), ternary (PLA-GB), and quaternary (PLA-GBC) composites are presented in Figure 2. Specifically, the TS and TM are presented in Figure 2(a) while the FS and FM are presented in Figure 2(b). It is evident from Figures 2(a,b) that incorporation of GF produced remarkable improvement in the tensile properties of PLA. The drastic increase in tensile properties of the PLA-G composite indicates that the incorporation of GF is very effective at improving the rigidity and strength of PLA.¹¹ Similarly, the flexural properties increment in the case of

PLA-G compared to PLA further demonstrates the positive influence of GF to enhance the rigidity of PLA.^{33,34} This is believed to have been greatly influenced by the high strength of GF, and the good dispersion of GF in the PLA matrix as presented in Figure 1(b).

It was observed that the tensile and flexural properties of the PLA-G composite decreased following the incorporation of Biostrong impact modifier and the CESA chain extender (Table 3), which suggests that the effect of reinforcement was more dominant compared to incorporation of additives, or probably due to reduced stiffness of PLA in the composites. Nevertheless, the TS, TM, FS, and FM values of the ternary and quaternary composites are higher than neat PLA. It is particularly worthy of note that whereas the incorporation of impact modifier led to noticeable reduction in tensile and flexural properties of the GF reinforced PLA composite, addition of chain extender helped to partially restore the tensile and flexural properties. The partial restoration in mechanical properties of the PLA-GBC system can be attributed to the fact that CESA is a chain extender based on a PLA carrier,³⁰ which helps to facilitate thermodynamic miscibility between CESA and PLA. Chain ends are known to act as stress concentration sites in composites. Therefore, CESA as a chain extender would facilitate the formation of branched macromolecules, which could invariably enhance the mechanical properties of PLA, even in reinforced composites.⁵ This is because the branches generally possess stronger binding forces that could help to produce improved mechanical performance.^{28,30}

The IS of PLA and the different composite categories are illustrated in Figure 3. It can be seen from the figure that the IS of the composites are higher than neat PLA. Incorporation of 10 wt% GF resulted in an increase in IS from 19 KJ/m² to about 25 KJ/m² which corresponds to

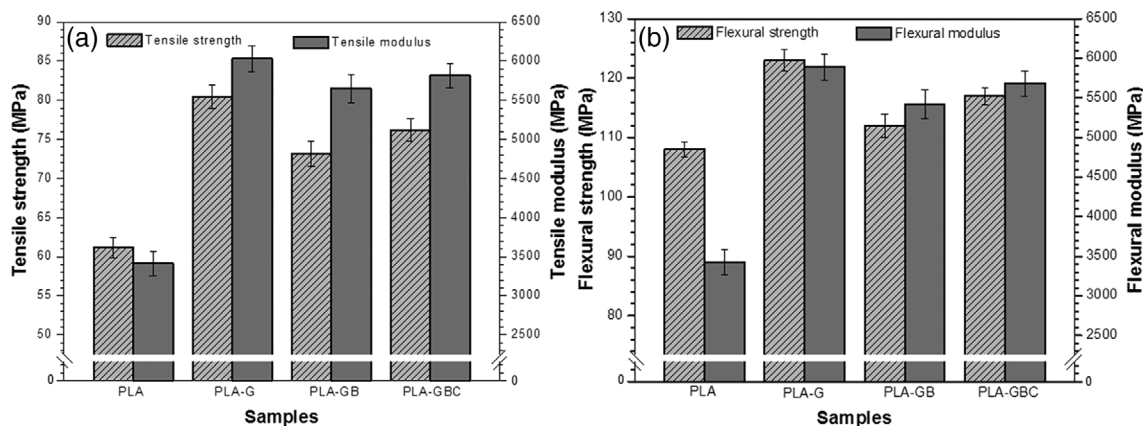
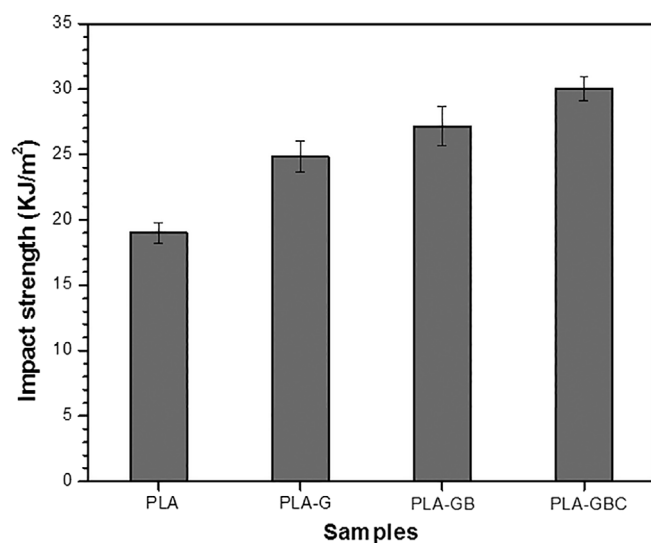


FIGURE 2 Tensile strength, tensile modulus, flexural strength, and flexural modulus of neat poly(lactic acid) (PLA), glass fiber (GF) reinforced PLA composite (PLA-G), GF reinforced ternary PLA composite containing BS (PLA-GB), and reinforced quaternary PLA composite containing BS and CESA (PLA-GBC)

TABLE 3 Summary of mechanical properties of PLA and the different composite categories

Sample code	TS (MPa)	TM (MPa)	FS (MPa)	FM (MPa)	IS (KJ/m ²)
PLA	61.3	3413	108	3420	19.2
PLA-G	80.4	6030	123	5890	24.8
PLA-GB	73.2	5652	112	5420	27.2
PLA-GBC	76.3	5816	117	5680	30.1

Abbreviations: FM, flexural modulus; FS, flexural strength; IS, impact strength; PLA, poly(lactic acid); TM, tensile modulus; TS, tensile strength.

**FIGURE 3** Impact strength of neat poly(lactic acid) (PLA), glass fiber (GF) reinforced PLA composite (PLA-G), GF reinforced ternary PLA composite containing BS (PLA-GB), and reinforced quaternary PLA composite containing BS and CESA (PLA-GBC)

an increase of about 31%. This can be attributed to the relatively uniform dispersion of GF in the PLA matrix as revealed by the SEM observation. This might have helped to arrest the possible initiation and propagation of crack as reported in a previous study.¹¹ In addition, this will facilitate improved stress transfer from the matrix to the reinforcing fillers, thereby increasing the IS.

Significantly, incorporation of the BS impact modifier produced a further increase in the IS of the PLA-G binary system as revealed by the higher IS of PLA-GB compared to PLA-G. This was further increased in the quaternary system (PLA-GBC) when CESA was incorporated into the PLA-GB ternary system. The SEM images presented in Section 3.1 shows that the interfacial interaction between PLA and GF in the composites is in the order PLA-G < PLA-GB < PLA-GBC. Invariably, the improved interface would raise the energy consumption during the pull out of fibers from the matrix, thereby resulting in higher IS. This explains the higher IS of the ternary (PLA-GB) and quaternary (PLA-GBC) composites, compared to the binary composite (PLA-G). Normally,

formation of branched structure following the incorporation of chain extenders could help to arrest the formation of cracks,³⁵ and this can be more effectively investigated from the IS of the composites. The IS values of the PLA-GBC composites as presented in Table 3 provides more evidence of the possible crack-arresting activities of the chain extender. This can be attributed to the formation of long branched chains, which could help to increase the IS by inhibiting the possible formation of cracks in either of two ways. First, the incorporation of CESA would help to increase the molecular weight, which will invariably reduce the number of chain ends through the production of branched structures.³⁰ Second, the thermodynamic miscibility of PLA and CESA as stated earlier would allow CESA to bind the reactive terminal ends of the larger macromolecule, thereby effectively transferring emerging microcracks to the newly formed stress-relieving surface structure.³⁰ This explains the notable increase in IS of the quaternary composite (PLA-GBC) compared to the other composites and neat PLA.

3.3 | FTIR spectroscopy

The FTIR spectra of neat PLA and the different composite categories such as the binary composite (PLA-G), ternary composite (PLA-GB), and the quaternary composite (PLA-GBC) are illustrated in Figure 4. As presented in the figure, some of the notable peaks common to all the samples include —OH stretching vibrations at the higher wavelength regions which is a characteristic of bonded —OH groups, the symmetric and asymmetric C—H stretching split peak around 2830–2999 cm⁻¹, the C=O stretching vibration peak at 1750 cm⁻¹ from carboxylic, ester, and acetyl groups, and the characteristic C—C symmetric stretching peak at 1454 cm⁻¹. In addition, the peak at 1376 cm⁻¹ is attributed to C—H symmetric deformation while the peak at 1168 cm⁻¹ is an attribute of C—O stretching, emanating from the carboxylic acid and ester components of PLA.^{36,37} It is significant that the incorporation of BS and CESA did not undesirably disrupt the skeletal structure of PLA. This can be attributed

to the good compatibility of between PLA and BS,¹³ as well as PLA and CESA.³⁰

The general structure of PLA, BS, and CESA are illustrated in Figure 5. It can be seen in the figure that both BS and CESA have epoxy group in the oxirane ring present in their structure. Interestingly, the epoxy group can thermodynamically react with carboxyl and hydroxyl groups of PLA. This is particularly favorable in the case of carboxyl groups where electrophilic reaction with epoxide can take place,³⁸ which has been confirmed in a previous study.²⁸ Therefore, these reactions are believed to have contributed to the increased interfacial interaction in the ternary and quaternary composites as discussed in the previous sections. It is expected that the presence of more epoxide groups would facilitate improved reaction. Hence, this might be the reason for increased interaction in the PLA-GBC composite

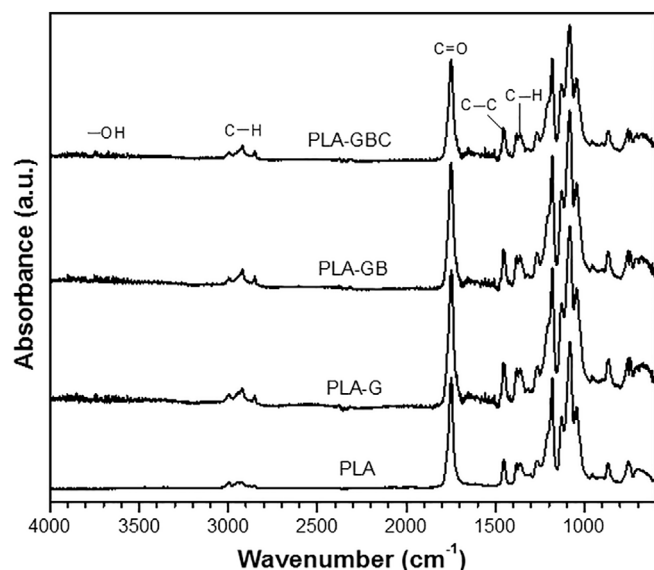


FIGURE 4 Fourier transform infrared spectra of neat poly(lactic acid) (PLA), glass fiber (GF)-reinforced PLA composite (PLA-G), GF reinforced ternary PLA composite containing BS (PLA-GB), and reinforced quaternary PLA composite containing BS and CESA (PLA-GBC)

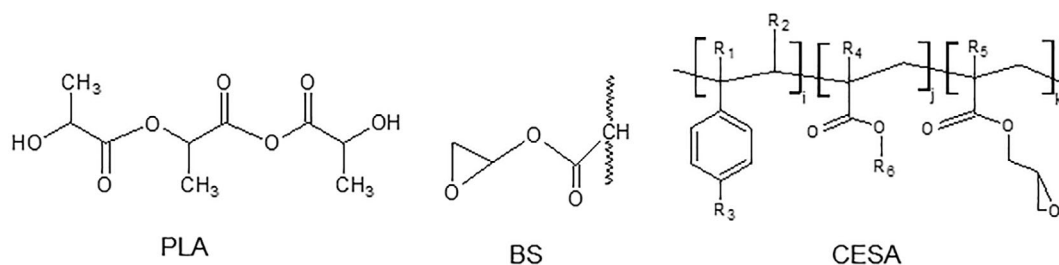


FIGURE 5 General structure of poly(lactic acid) (PLA), BS, and CESA, where R_1 – R_5 could be H, CH_3 , a higher alkyl group, or their combinations, while R_6 is an alkyl group, and i , j , and k are between 1 and 20 each

compared to the PLA-GB composite as confirmed through SEM, and this could be responsible for the higher mechanical performance of the quaternary composite compared to the ternary composite.

3.4 | Thermogravimetric analysis

The TGA curves of the samples are illustrated in Figure 6 (a) while the derivative thermogravimetry (DTG) curves are illustrated in Figure 6(b). As can be seen in Figure 6 (a), the TGA and DTG curves of all the samples follow similar pattern with one major degradation peak and an additional shoulder peak for the samples containing BS (Figure 6(b)) Similar observation was reported previously for impact modified PLA composites containing impact BS impact modifier.¹³ The degradation onset temperature (T_{onset}) and thermal degradation temperature (T_d) of the samples can be obtained from the DTG curve. However, the temperature at 50% weight loss (T_{50}) of the sample may be considered as an indicator of structural destabilization to represent the T_d . Summary of the degradation properties of the samples is presented in Table 4. As can be seen in Table 4, the T_{onset} and T_d of the composites are higher than neat PLA. This indicates higher thermal stability of the composites compared to PLA. Actually, the incorporation of GF produced very little improvement in thermal stability of PLA, perhaps due to low interfacial interactions between the PLA matrix and GF as revealed by the SEM image in Figure 1(b). This might have allowed higher heat penetration into the interface of the composite, thereby causing structural destabilization of the PLA structural framework in the PLA-G composite. On the other hand, it might be due to degradation of the PLA end chains,²⁸ which might have been left exposed by the poor interaction between GF and PLA.

The incorporation of BS impact modifier into the binary composite helped to raise the thermal stability of PLA in the resulting ternary composite, which may be accrued to improved interfacial interaction between the fiber and the matrix. This was further improved by the

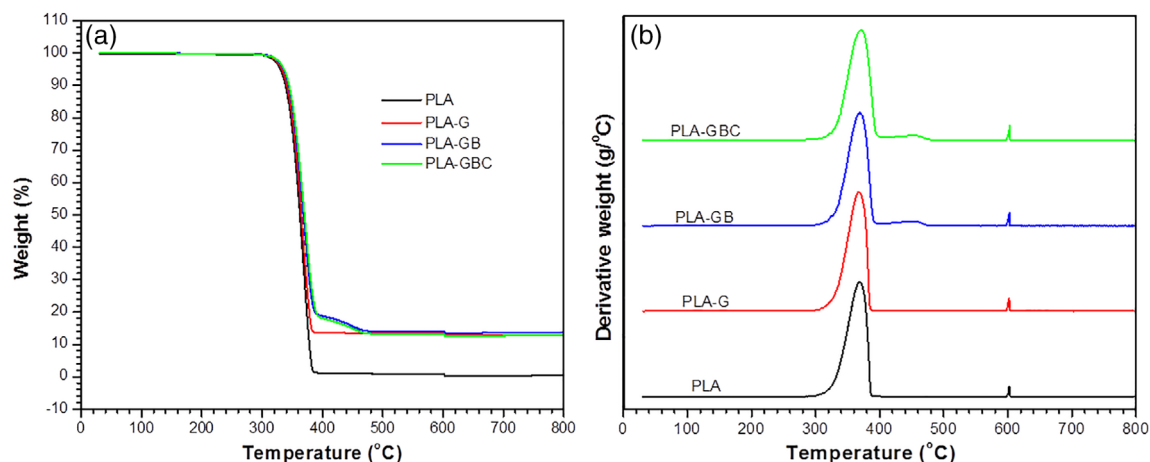


FIGURE 6 (a) Thermogravimetric analysis curves and (b) DTG curves of neat poly(lactic acid) (PLA), glass fiber (GF)-reinforced PLA composite (PLA-G), GF reinforced ternary PLA composite containing BS (PLA-GB), and reinforced quaternary PLA composite containing BS and CESA (PLA-GBC) [Color figure can be viewed at wileyonlinelibrary.com]

TABLE 4 Thermal properties of PLA and the different composite categories

Sample	TGA			DSC			
	Code	T_{onset} (°C)	T_d (°C)	Residue (%) at $T \geq 700^\circ\text{C}$	T_g (°C)	T_c (°C)	T_m (°C)
PLA	309	363	0.3	60.63	114.21	149.17	24.73
PLA-G	313	364	12.8	60.69	120.10	149.76	33.91
PLA-GB	313	368	12.6	61.58	129.56	153.27	29.27
PLA-GBC	315	370	13.2	61.97	117.49	154.89	40.42

Abbreviations: DSC, differential scanning calorimetry; PLA, poly(lactic acid); TGA, thermogravimetric analysis.

incorporation of CESA chain extender, perhaps due to restorative effects of CESA on the degrading chains of PLA, as reported in a similar study.⁵ It is well known that degradation mainly occurs at the reactive chain ends of the polymer.²⁸ Therefore, the reaction between CESA chain extender and the reactive chain ends of PLA would lead to formation of longer branched chains, which will invariably reduce the degradation rate. This is believed to be responsible for the significant increase in T_d of the quaternary composite, compared to neat PLA and the other composite categories. Specifically, the T_d of the quaternary composite (PLA-GBC) increased by 7°C compared to neat PLA which is highly desirable in structural applications. The amount of residue at 700°C for each of the samples is included in Table 4. It is evident from the residual weight of the samples that the incorporation of filler and additives actually contributed to the thermal stability of the composites.

3.5 | DSC analysis

The DSC curves of PLA and the different composite categories during the second heating step are illustrated in

Figure 7, which reveals three distinct successive transition stages. The first transition represents the endothermic glass transition temperature, T_g , the second transition which is an exothermic transition represents the crystallization temperature, T_c while the third transition represents the endothermic melting temperature, T_m . The DSC parameters of the samples are included in Table 4. As can be seen in Figure 7 and as presented in Table 4, there is no significant shift in the T_g of PLA after the incorporation of GF. However, incorporation of BS and CESA caused the T_g of PLA in the resulting ternary (PLA-GB) and quaternary (PLA-GBC) composites to slightly shift towards the higher temperature zone. It is well known that close to the T_g of polymer composites, the molecular chains of the polymer becomes more flexible, thereby gaining mobility.³⁹ Therefore, the negligible increase in T_g of PLA in the PLA-G composite suggests that the incorporation of GF did not sufficiently restrict the mobility of PLA chains in the composite.

In a previous study, incorporation of BS impact modifier was reported to lubricate PLA chains, thereby enhancing chain mobility, which resulted in lower T_g of the PLA-BS composites compared to neat PLA.¹³

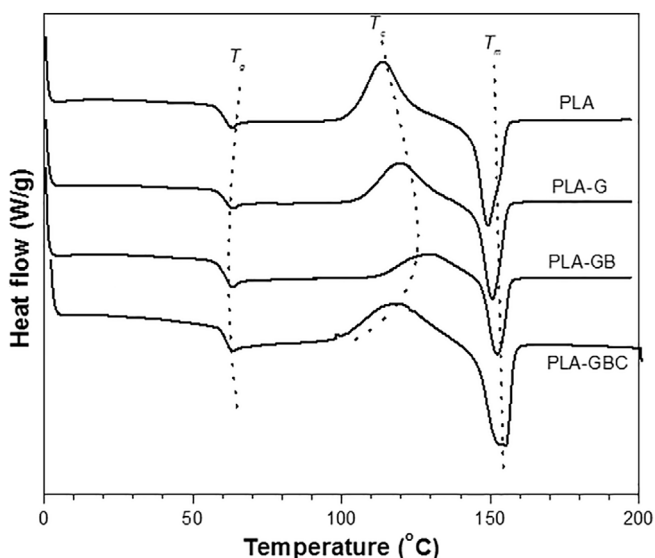


FIGURE 7 Differential scanning calorimetric thermograms of neat poly(lactic acid) (PLA), glass fiber (GF)-reinforced PLA composite (PLA-G), GF reinforced ternary PLA composite containing BS (PLA-GB), and reinforced quaternary PLA composite containing BS and CESA (PLA-GBC)

However, in this study, despite the expected increase in chain mobility of PLA following the incorporation of BS, the T_g of PLA-GB composite can be seen to shift upwards, indicating higher restriction to chain mobility. This is believed to be due to the increased interaction between PLA and GF, probably because BS was able to lubricate the PLA chains, thereby allowing more effective insertion of GF such that the interaction between PLA and GF is enhanced. As such, the GF would be able to effectively restrict the chain mobility of PLA in the composites. This is also evident through the reduced number of fiber pull out and debonding sites in the SEM image of the PLA-GB composites presented in Figure 1(c). Incorporation of CESA into the BS containing composite can be seen to further shift the T_g to the right side which may be attributed to possible delay in chain mobility due to the chain extension activities of CESA,⁵ as well as improved interfacial interaction between PLA and GF as revealed by the SEM image in Figure 1(d).

Generally, the incorporation of fillers into semi crystalline matrices such as PLA would lead to a right or left shift in the T_c depending on the nucleation ability of the filler. The wide crystallization peaks of neat PLA as illustrated in Figure 7 indicates slow crystallization and it is evident in Figure 7 and Table 4 that incorporation of GF could not induce sufficient heterogeneous nucleation in the PLA-G system. This may possibly be due to poor interfacial interaction between PLA and GF. It might also be due to the macrosized of GF,¹⁰ which could not

effectively initiate the formation of new crystals or support the growth of existing spherulites. These explain the reason for the negligible increase in T_m of PLA-G composite. Incorporation of BS into the binary composite further shifted the T_c peak to the right side and this is attributed to the rubbery nature of BS,¹³ which might have hampered proper nucleation activities in the composite. This suggests that BS might have mainly facilitated the insertion of GF into the PLA matrix without necessarily enhancing heterogeneous nucleation.

However, it is noteworthy that improved interaction between PLA and GF following the incorporation of BS helped to shift the T_m of the resulting ternary composite (PLA-GB) by about 4°C as presented in Table 4. Afterwards, a significant left shift in the T_c can be seen in the PLA-GBC system which is an indication of increased nucleation activities in the composite,^{39,40} accrued to the incorporation of CESA. Although similar observation was reported in a previous study where CESA was incorporated into PLA without any reinforcing filler,³⁰ it is interesting to note here that same effect can be achieved in reinforced PLA. This is an indication that the chain extender can effectively accelerate crystal structure formation, even in reinforced PLA composites. Going forward, this account for the right shift in the T_m of the PLA-GBC system perhaps due to the creation of small and less perfect crystals, which are known to generally melt at higher temperatures than the more perfect crystals.³⁹

In order to further investigate the crystallization activities in the different samples, the degree of crystallinity ($X_{DSC}\%$) was calculated as described in Section 2.2.8, using Equation (1). The $X_{DSC}\%$ of the samples are included in Table 4. It is evident from Table 4 that the incorporation of CESA did not only act as heterogeneous nucleation sites for the initiation of new crystallites, but it might probably have facilitated the growth of existing spherulites which invariably resulted in higher $X_{DSC}\%$ of the quaternary system (PLA-GBC). Indeed, this might have contributed to the partial restoration of mechanical properties in the PLA-GBC composite compared to the PLA-GB system as discussed in Section 3.2.

3.6 | Dynamic mechanical properties

The thermomechanical properties of PLA and the different composite systems were investigated through DMA analysis. The variation of storage modulus (E') of the samples with temperature is illustrated in Figure 8(a). It can be seen in the figure that below the glass transition temperature, T_g , of the samples, their E' remained almost unchanged. However, a drastic fall in the E' can be seen

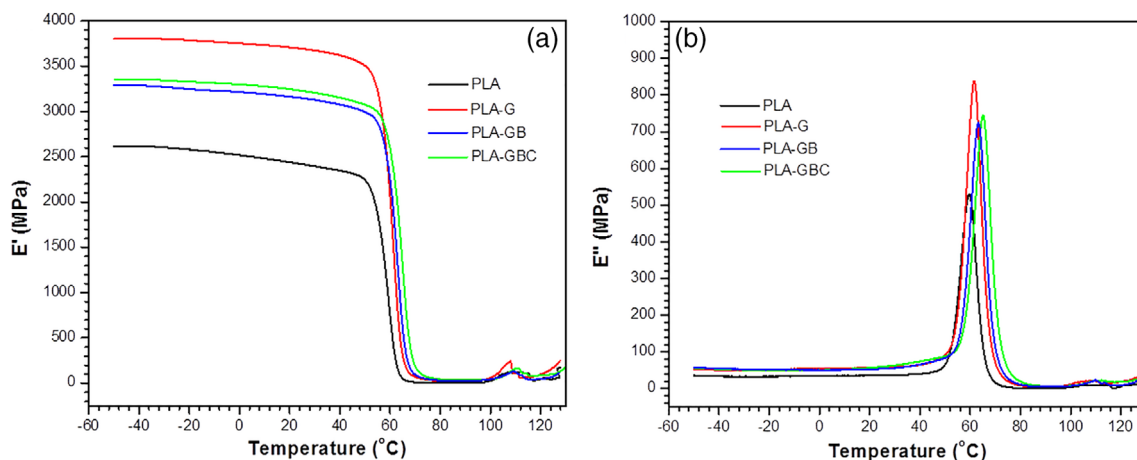


FIGURE 8 (a) Storage modulus and (b) loss modulus curves of neat poly(lactic acid) (PLA), glass fiber (GF)-reinforced PLA composite (PLA-G), GF reinforced ternary PLA composite containing BS (PLA-GB), and reinforced quaternary PLA composite containing BS and CESA (PLA-GBC) [Color figure can be viewed at wileyonlinelibrary.com]

in the T_g region. In addition, the figure shows that the E' of PLA is lower than the composite systems over the entire temperature range. Different factors can influence the variation in E' of composites. These include factors such as type of matrix, type of reinforcement, filler dispersion, and fiber-matrix interfacial interaction.^{41,42} Therefore, the higher E' of the composites can be accrued to the stiffness imposed on the PLA matrix by the reinforcing filler, perhaps due to the very high modulus of GF. The incorporation of BS resulted in an initial drop in the E' of the PLA-G composites as evident in the lower E' value of PLA-GB illustrated in Figure 8(a). This may be attributed to the rubbery nature of BS, which might have interrupted the stiffening activities of the GF. Notwithstanding the E' of the PLA-GB composite is higher than neat PLA, which might be due to interfacial interactions between PLA and GF, following the incorporation of BS, which helped to facilitate stress transfer from the matrix to the filler. On the other hand, incorporation of CESA helped to increase the E' of the PLA-GB composite as can be seen in the higher E' value of PLA-GBC compared to PLA-GB in Figure 8(a). This indicates that the incorporation of CESA helped to enhance the ability of PLA to endure mechanical constraints through the process of recoverable viscoelastic deformation.

The loss modulus (E'') curves of the samples are illustrated in Figure 8(b). It can be seen in the figure that as temperature increases, the E'' of the samples also increases gradually with a sharp increase around the T_g region which attained a climax (indicating maximum mechanical energy dissipation). This was followed by a subsequent decrease as the temperature was further increased due to increased polymer chain mobility at

higher temperature. Obviously, the peak of the E'' curve of PLA is lower than all the composites. This has been previously attributed to higher chain segment in the free volume of the matrix, which might have inhibited the chain relaxation processes within the composites.⁴³ In addition, the higher curve peaks of the composites suggests higher energy absorption, as a result of increases energy dissipation sites which might have emanated from the larger surface areas created within the composites by the incorporation of filler and other components. Actually, strong interface within a composite system may be assessed by the energy dissipation tendency of the composite. Therefore, the loss modulus and the interfacial interaction within a composite are closely related, and this is often investigated through the loss factor ($\tan \delta$), otherwise called the damping parameter of the composite.⁴⁴

Generally, the $\tan \delta$ is obtained as the ratio of the energy dissipated (E'') to the energy stored (E'). In addition to viscoelastic energy dissipation, it has been previously reported that the damping coefficient ($\tan \delta$) may be influenced by the concentration of shear stress within a composite.⁴⁵ Therefore, $\tan \delta$ largely depends on the degree of interaction between the filler and the matrix, where good interaction will produce low $\tan \delta$ values as a result of reduced polymer chain mobility.⁴⁵ The $\tan \delta$ curves of PLA and the different composite systems are illustrated in Figure 9. It can be seen in the figure that the $\tan \delta$ of the composites are lower than neat PLA, which is a good indication of improved load bearing capacity. Among the composites, the binary composite (PLA-G) has the highest $\tan \delta$ which is expected considering the poor interface of the PLA-G system as revealed through the SEM image in Figure 1. Similarly, the $\tan \delta$

values of the PLA-GB and PLA-GBC composites align with the SEM observation.

In another vein, $\tan \delta$ curve is well known for its suitability to accurately determine the T_g . The T_g can be obtained from the $\tan \delta$ curve as the temperature at which the $\tan \delta$ reached a climax. The T_g obtained from the $\tan \delta$ curve of the different samples with their corresponding $\tan \delta$ peak values are summarized in Table 5. Based on the result presented in Table 5, it can be inferred that the incorporation of GF, BS, and CESA only slightly modified the T_g of PLA. It is noteworthy that this observation conforms to the result obtained from the DSC analysis. Therefore, it is suffice to say that the incorporation of GF, BS, and CESA presents more influence on the $\tan \delta$ peak value compared to the T_g . As such, the level of interfacial interactions within the different composite systems was further investigated following a method previously described in the literature.⁴³ This was assessed by calculating the effectiveness coefficient. The effectiveness coefficient, C , is calculated as the ratio of the composite's E' (in the glass and rubbery regions), to the E' of the neat

matrix (in the glassy and rubbery regions). The effectiveness coefficient was measured using Equation (2).

$$\text{Effectiveness coefficient } (C) = \frac{E'_g/E'_r(\text{composite})}{E'_g/E'_r(\text{matrix})}, \quad (2)$$

where E'_g and E'_r are the storage modulus in the glassy rubbery regions, respectively. Generally, a higher C value is an indication of low effectiveness whereas higher effectiveness would produce a low C value.⁴³ The calculated C values of the samples are included in Table 5. It can be seen in Table 5 that the effectiveness of GF to reinforce PLA was improved by the incorporation of BS, which was subsequently improved further by the addition of CESA. Therefore, it can be inferred that while GF supplies the necessary strength and modulus to reinforce PLA, incorporation of BS and CESA could help to improve the interfacial interactions so as to avoid undesirable failure at the fiber-matrix interface during use.

4 | CONCLUSIONS

Different categories of reinforced PLA composites such as binary, ternary, and quaternary composites were prepared, using GF as the reinforcing filler. Biomax® Strong 120 impact modifier was used to achieve good toughening and impact properties of the composites. In addition, CESA-extend which is a chain extender was added to produce the quaternary composite. The concurrent effects of these additives on the toughness, spectroscopic, crystallization, mechanical, thermal, and thermomechanical properties of the resulting composites were investigated. It was observed that incorporation of 10 wt% GF helped to improve the mechanical performance of PLA which was attributed to the higher strength and modulus GF. Despite this, the chain mobility of PLA could not be significantly restricted by GF. In addition, the crystallization activity in the PLA-GF composite was poor as confirmed through DSC analysis.

On the other hand, morphological and spectroscopic analysis revealed that the interaction between GF and PLA was significantly enhanced by the incorporation of impact modifier and the chain extender. This was more

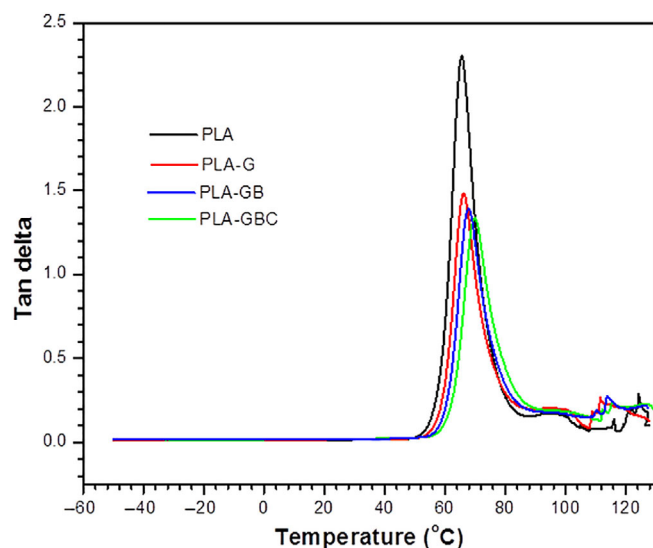


FIGURE 9 Tan delta curves of neat poly(lactic acid) (PLA), glass fiber (GF)-reinforced PLA composite (PLA-G), GF-reinforced ternary PLA composite containing BS (PLA-GB), and reinforced quaternary PLA composite containing BS and CESA (PLA-GBC) [Color figure can be viewed at wileyonlinelibrary.com]

Sample code	Max $\tan \delta$ peak value	T_g (°C)	Effectiveness coefficient (C)
PLA	2.30	65.58	1
PLA-G	1.48	65.96	0.50
PLA-GB	1.39	66.49	0.37
PLA-GBC	1.34	67.69	0.31

TABLE 5 Damping parameters and effectiveness coefficient, C , of poly(lactic acid) (PLA) and the different composite categories

evident in the quaternary composite, which resulted in significant improvement in mechanical, thermal, and thermomechanical properties. Specifically, the crystallinity, IS, and FM of PLA in the quaternary composite were increased by 58%, 63%, and 66%, respectively compared to neat PLA. In fact, DSC analysis revealed that incorporation of CESA did not only act as heterogeneous nucleation sites for the initiation of new crystallites, also facilitated the growth of existing spherulites, which invariably resulted in higher X_{DSC} of the quaternary system (PLA-GBC). Invariably, this contributed to the partial restoration of mechanical properties in the quaternary (PLA-GBC) composite compared to the ternary (PLA-GB) system. Furthermore, the damping and effectiveness coefficient of the PLA-GF composite were notably reduced by the simultaneous impact modification and chain extension of the reinforced composites. Therefore, it can be inferred that while GF supplies the necessary strength and modulus to reinforce PLA, incorporation of BS and CESA could help to toughen, improve the interfacial interactions, and limit thermal degradation so as to avoid undesirable failure at the fiber-matrix interface during use, especially in structural and engineering composites.

ACKNOWLEDGMENT

The authors appreciate the Hessen State Ministry of Higher Education, Germany for the financial support, and the Institute of Materials Engineering, Universität Kassel for allowing part of the research to be conducted in their laboratory. The first author would also like to thank the Universiti Sains Malaysia for the Postdoctoral Fellowship and the Universiti Malaysia Pahang for their contribution.

ORCID

John Olabode Akindoyo  <https://orcid.org/0000-0002-7701-123X>

REFERENCES

- [1] R. Geyer, J. R. Jambeck, K. L. Law, *Sci. Adv.* **2017**, *3*, e1700782.
- [2] D. K. Schneiderman, M. A. Hillmyer, *Macromolecules* **2017**, *50*, 3733.
- [3] J. O. Akindoyo, N. H. Ismail, M. Mariatti, *Polym. Test.* **2019**, *80*, 106140.
- [4] S. K. Sansaniwal, M. A. Rosen, S. K. Tyagi, *Renew. Sustain. Energy Rev.* **2017**, *80*, 23.
- [5] A. Jaszkiwicz, A. Meljon, A. K. Bledzki, *Polym. Compos.* **2018**, *39*, 1716.
- [6] R. M. Rasal, A. V. Janorkar, D. E. Hirt, *Prog. Polym. Sci.* **2010**, *35*, 338.
- [7] L. T. Lim, R. Auras, M. Rubino, *Prog. Polym. Sci.* **2008**, *33*, 820.
- [8] V. Nagarajan, A. K. Mohanty, M. Misra, *ACS Sustainable Chem. Eng.* **2016**, *4*, 2899.
- [9] Y. Chen, L. M. Geever, J. A. Killion, J. G. Lyons, C. L. Higginbotham, D. M. Devine, *Polym.-Plast. Technol. Eng.* **2016**, *55*, 1057.
- [10] G. Wang, D. Zhang, B. Li, G. Wan, G. Zhao, A. Zhang, *Int. J. Biol. Macromol.* **2019**, *129*, 448.
- [11] G. Wang, D. Zhang, G. Wan, B. Li, G. Zhao, *Polymer* **2019**, *181*, 121803.
- [12] K. Hamad, M. Kaseem, M. Ayyoob, J. Joo, F. Deri, *Prog. Polym. Sci.* **2018**, *85*, 83.
- [13] J. O. Akindoyo, M. D. H. Beg, S. Ghazali, H. P. Heim, M. Feldmann, *Compos. A: Appl. Sci. Manuf.* **2018**, *107*, 326.
- [14] K.-t. Lau, P.-y. Hung, M.-H. Zhu, D. Hui, *Composites, Part B* **2018**, *136*, 222.
- [15] N. Graupner, A. S. Herrmann, J. Müssig, *Compos. A: Appl. Sci. Manuf.* **2009**, *40*, 810.
- [16] S. Lv, J. Gu, H. Tan, Y. Zhang, *J. Clean. Prod.* **2018**, *203*, 328.
- [17] P. Georgiopoulos, E. Kontou, G. Georgousis, *Compos. Commun.* **2018**, *10*, 6.
- [18] K.-Y. Lee, J. J. Blaker, A. Bismarck, *Compos. Sci. Technol.* **2009**, *69*, 2724.
- [19] H. Xiu, X. Qi, Z. Liu, Y. Zhou, H. Bai, Q. Zhang, Q. Fu, *Compos. Sci. Technol.* **2016**, *127*, 54.
- [20] S. D. Varsavas, C. Kaynak, *Mater. Today Commun.* **2018**, *15*, 344.
- [21] Y. Qin, Y. Xu, L. Zhang, G. Zheng, X. Yan, K. Dai, C. Liu, C. Shen, Z. Guo, *Polymer* **2016**, *100*, 111.
- [22] B. Yu, C. Geng, M. Zhou, H. Bai, Q. Fu, B. He, *Composites, Part B* **2016**, *92*, 413.
- [23] G. D. Goh, V. Dikshit, A. P. Nagalingam, G. L. Goh, S. Agarwala, S. L. Sing, J. Wei, W. Y. Yeong, *Mater. Des.* **2018**, *137*, 79.
- [24] C. Zhu, I. Ahmed, A. Parsons, Y. Wang, C. Tan, J. Liu, C. Rudd, X. Liu, *Polym. Compos.* **2018**, *39*, E140.
- [25] T. P. Sathishkumar, S. Satheeshkumar, J. Naveen, *J. Reinf. Plast. Compos.* **2014**, *33*, 1258.
- [26] V. Cech, E. Palesch, J. Lukes, *Compos. Sci. Technol.* **2013**, *83*, 22.
- [27] R. Al-Ittry, K. Lamnawar, A. Maazouz, *Polym. Degrad. Stab.* **2012**, *97*, 1898.
- [28] N. Najafi, M. C. Heuzey, P. J. Carreau, P. M. Wood-Adams, *Polym. Degrad. Stab.* **2012**, *97*, 554.
- [29] A. Jaszkiwicz, A. K. Bledzki, A. Duda, A. Galeski, P. Franciszczak, *Macromol. Mater. Eng.* **2014**, *299*, 307.
- [30] A. Jaszkiwicz, A. K. Bledzki, R. van der Meer, P. Franciszczak, A. Meljon, *Polym. Bull.* **2014**, *71*, 1675.
- [31] S. D. Varsavas, C. Kaynak, *Compos. Commun.* **2018**, *8*, 24.
- [32] M. A. Sawpan, K. L. Pickering, A. Fernyhough, *Compos. A: Appl. Sci. Manuf.* **2011**, *42*, 310.
- [33] J. Karger-Kocsis, H. Mahmood, A. Pegoretti, *Prog. Mater. Sci.* **2015**, *73*, 1.
- [34] J. Sliseris, L. Yan, B. Kasal, *Composites, Part B* **2016**, *89*, 143.
- [35] S. Mortazavian, A. Fatemi, *Int. J. Fatigue* **2015**, *70*, 297.
- [36] J. O. Akindoyo, M. D. H. Beg, S. Ghazali, M. R. Islam, *J. Appl. Polym. Sci.* **2015**, *132*, 42784.
- [37] J. O. Akindoyo, M. D. H. Beg, S. B. Ghazali, M. R. Islam, A. A. Mamun, *Polym.-Plast. Technol. Eng.* **2015**, *54*, 1321.
- [38] H. Inata, S. Matsumura, *J. Appl. Polym. Sci.* **1985**, *30*, 3325.

- [39] J. O. Akindoyo, M. D. H. Beg, S. Ghazali, H. P. Heim, M. Feldmann, *Compos. A: Appl. Sci. Manuf.* **2017**, *103*, 96.
- [40] J. Liuyun, X. Chengdong, J. Lixin, C. Dongliang, L. Qing, *Mater. Res. Bull.* **2013**, *48*, 1233.
- [41] H. Essabir, A. Elkhaoulani, K. Benmoussa, R. Bouhfid, F. Z. Arrakhiz, A. Qaiss, *Mater. Des.* **2013**, *51*, 780.
- [42] H. Essabir, E. Hilali, A. Elgharad, H. El Minor, A. Imad, A. Elamraoui, O. Al Gaoudi, *Mater. Des.* **2013**, *49*, 442.
- [43] D. Romanzini, A. Lavoratti, H. L. Ornaghi, S. C. Amico, A. J. Zattera, *Mater. Des.* **2013**, *47*, 9.
- [44] A. Etaati, S. Pather, Z. Fang, H. Wang, *Composites, Part B* **2014**, *62*, 19.
- [45] K. V. Krishna, K. Kanny, *Composites, Part B* **2016**, *104*, 111.

How to cite this article: Akindoyo JO, Beg MDH, Ghazali S, Heim HP, Feldmann M, Mariatti M. Simultaneous impact modified and chain extended glass fiber reinforced poly(lactic acid) composites: Mechanical, thermal, crystallization, and dynamic mechanical performance. *J Appl Polym Sci.* 2021; 138:e49752. <https://doi.org/10.1002/app.49752>